FLEXIBLE BOUNDARY CONDITIONS FOR A BOUSSINESQ-TYPE WAVE MODEL

Mart Borsboom[1], Jacco Groeneweg[1], Neelke Doorn[1], and Marcel van Gent[1]

Abstract: A procedure is presented for the dynamic handling of the boundaries of Boussinesq-type wave models that enables to control the reflection properties. The main purpose of the procedure is the reduction of spurious reflections at open boundaries. The procedure also allows, however, the modeling of partial reflection at closed boundaries. The approach chosen takes into account the effect of wave direction, wave period, and wave height, in order that irregular waves, waves at arbitrary angles, and steep waves can all be handled properly. An innovative aspect of the developed method is that it can equally well be used for strongly dispersive waves, since besides the angle of outgoing waves also the celerity is determined dynamically. The results presented demonstrate the feasibility of the approach; reflection coefficients of only about 1% are obtained for regular waves, varying angle, period, as well as steepness.

INTRODUCTION

For many computational models the design of suitable boundary conditions is a far from trivial task. In a wave model, the computational domain is usually embedded in a larger area (e.g., a sea) and separated from its surroundings by artificial boundaries. Ideally, these boundaries are 'transparent' or 'open', i.e., waves should be able to propagate freely across without generating spurious effects. Likewise, the conditions applied at physical, closed boundaries should not lead to spurious wave reflections either, but model the physical reflection that may be total (vertical wall) or partial (beach, breakwater, dam, jetty). Since the wave propagation properties depend on frequency, direction, and amplitude, a boundary procedure suitable for a Boussinesq-type wave model should take account of all these effects in a proper way.

The problems associated with boundary conditions can to some extent be avoided by applying absorbing layers. The wave absorption must increase slowly toward the boundary to prevent strongly non-uniform wave behavior that may lead to spurious reflections from inside the absorbing layer. As a result, a fairly large area may have to be added to the computational domain to obtain sufficient wave damping. Even

[1] WL|Delft Hydraulics, P.O. Box 177, 2600 MH Delft, The Netherlands
E-mail: mart.borsboom@wldelft.nl, jacco.groeneweg@wldelft.nl, neelke.doorn@wldelft.nl, marcel.vangent@wldelft.nl

though the additional computational costs may be acceptable, there may simply be not enough room to apply an absorbing layer. This occurs typically at boundaries formed by a structure whose width is small compared to a typical wavelength (e.g., a breakwater).

Wei et al. (1999) propose an interesting technique to avoid boundary conditions altogether. They place absorbing layers at all boundaries and generate the incident wave by adding a source term to the model equations. To ensure sufficient numerical accuracy, the source term needs to be a smooth function that extends over several grid points. So besides additional space for the absorbing layers, another area needs to be added to the computational domain for the source term. Linear wave theory is used to determine the source amplitude, and wave spectra are generated by superposition.

There are several reasons, however, to prefer genuine boundary conditions, provided a technique is available to avoid the excessive generation of spurious waves at boundaries. Using genuine boundary conditions, the computational domain does not have to be extended to create space for absorbing layers or source terms, and the modeling of structures of small width also becomes possible. Third, the possibility of modeling partial reflection becomes available, and the use of nonlinear wave theory to correct the specification of large-amplitude incident waves for nonlinear effects is fairly straightforward (Madsen and Sørensen 1993). Finally, it allows to use the model in a multi-domain approach, coupling different models in different subdomains through an exchange of boundary conditions at the interfaces.

Most developments on absorbing or weakly reflecting boundary conditions aim at minimizing reflections by optimizing the conditions using fixed coefficients. This type of boundary conditions works optimally only for the wave component(s) it is designed for. A review of techniques to improve their performance and extend their range of applicability can be found in (Givoli 1991). Very low spurious reflections can be obtained with the more elaborate techniques, but only for linear waves, while their complexity makes it difficult to apply them in a general-purpose wave model.

The alternative is a dynamic boundary condition, with coefficients that adapt themselves automatically to the local wave pattern at the boundary. This idea has successfully been developed for linear long waves and for shallow-water waves in resp. (Luchini and Tognaccini 1996) and (Van Dongeren and Svendsen 1997), where it was sufficient to determine only the angle of the outgoing wave from the wave solution. We have extended this type of boundary procedure for a Boussinesq-type model, where besides the angle also the celerity of the outgoing wave needs to be determined in order to include the effect of dispersion. We were also able to develop a more general framework which allows to compensate for nonlinear effects due to wave steepness and can be used for the modeling of partial reflection as well. The procedure is presented for the Boussinesq-type model TRITON of WL|Delft Hydraulics, but can be developed for other Boussinesq-type models as well. It has been used to specify weakly reflecting boundary conditions in simulations of regular waves at different frequencies, angles, and wave amplitudes. The results show that the method is capable of absorbing outgoing waves almost completely; very low reflection coefficients of only about 1% were observed.

THE BOUSSINESQ-TYPE MODEL

The Boussinesq-type wave model that we consider is the model recently developed at WL|Delft Hydraulics. By using the freedom that exists within the Boussinesq-type modeling approach, model equations were derived that express the conservation of both depth-integrated mass and depth-integrated momentum (Borsboom et al. 2000; Borsboom et al. 2001):

$$\frac{\partial H}{\partial t} + \nabla \cdot (H\overline{\mathbf{u}}) = 0 \;, \tag{1}$$

$$\frac{\partial H\overline{\mathbf{u}}}{\partial t} + \nabla \cdot (H\overline{\mathbf{u}}\,\overline{\mathbf{u}}) + g\nabla\left(\frac{1}{2}\widetilde{H}^2\right) = \mathbf{S}_m \;. \tag{2}$$

The unknowns of these equations are depth-averaged horizontal velocity vector $\overline{\mathbf{u}}$ and total water depth H that is the sum of water elevation ζ and water depth h. Auxiliary unknown $\widetilde{H}$ is obtained from:

$$\widetilde{H} - \alpha H^2\nabla^2\widetilde{H} = H - \left(\alpha - \frac{1}{3}\right) H^2\nabla^2 H + S_d \;. \tag{3}$$

Linear dispersion is modeled up to $O((kh)^6)$, with k a typical wave number, by taking parameter α equal to 0.4. In practice slightly lower values of α are used to extend the range of applicability of the model to higher values of kh. The terms $\mathbf{S}_m$ and S_d in respectively momentum equation (2) and dispersion equation (3) depend on the bottom slope and vanish for a uniform bottom. Since the effect of a sloped bottom is small over short distances, these terms are irrelevant in the analysis of the local wave patterns at the boundaries. In the present study it therefore suffices to consider them as source terms.

WAVE ANALYSIS

To analyse the wave dynamics at a boundary, the local *variation* of the solution of the Boussinesq-type model is decomposed in a number of components:

$$\begin{aligned} \partial H &= \sum \partial H_i = \sum Z_i\, f_i\,(\mathbf{k}_i \cdot \mathbf{x} - \omega_i t) \;, \\ \partial\overline{\mathbf{u}} &= \sum \partial\overline{\mathbf{u}}_i = \sum \overline{\mathbf{U}}_i\, f_i\,(\mathbf{k}_i \cdot \mathbf{x} - \omega_i t) \;, \end{aligned} \tag{4}$$

with the $f_i(\xi)$ normalized functions ($-1 \le f_i(\xi) \le 1$) oscillating at a normalized period of 2π. In a linear decomposition one would consider the solution as such, the $f_i(\xi)$ would be taken equal to $\sin(\xi + \phi_i)$ with the ϕ_i the phase of the components, and the variables in the right-hand sides of (4) would be constants. Here, we decompose the variation of the solution, the $f_i(\xi)$ are allowed to contain higher-order components of the form $\sin(n\xi), n = 2, 3, \ldots$, while the amplitudes Z_i and $\overline{\mathbf{U}}_i$, the wave number vectors $\mathbf{k}_i$, and the wave frequencies ω_i are allowed to vary smoothly in space and in time:

$$\begin{aligned} &|\nabla Z_i| \ll |\mathbf{k}_i|\,|Z_i| \;,\; \left|\nabla\overline{\mathbf{U}}_i\right| \ll |\mathbf{k}_i|\left|\overline{\mathbf{U}}_i\right| \;,\; |\nabla\mathbf{k}_i| \ll |\mathbf{k}_i|\,|\mathbf{k}_i| \;,\; |\nabla\omega_i| \ll |\mathbf{k}_i|\,|\omega_i| \;, \\ &\left|\frac{\partial Z_i}{\partial t}\right| \ll |\omega_i|\,|Z_i| \;,\; \left|\frac{\partial\overline{\mathbf{U}}_i}{\partial t}\right| \ll |\omega_i|\left|\overline{\mathbf{U}}_i\right| \;,\; \left|\frac{\partial\mathbf{k}_i}{\partial t}\right| \ll |\omega_i|\,|\mathbf{k}_i| \;,\; \left|\frac{\partial\omega_i}{\partial t}\right| \ll |\omega_i|\,|\omega_i| \;, \end{aligned} \tag{5}$$

where the vertical bars $|\cdot|$ denote suitable norms to measure the magnitude of the variables.

The idea of decomposition (4) is to capture most of the local variation in space and in time in the functions $f_i(\xi)$, using the smallest number of components possible. For example, a narrow-banded, long-crested wave spectrum can now be represented locally by a single nonlinear wave component, instead of by the sum over a large number of linear, constant-coefficient wave components.

Besides (4) we need a decomposition of the third term in the left-hand side of (2):

$$g\nabla\left(\frac{1}{2}\widetilde{H}^2\right) = \sum c_i^2 \nabla H_i \ , \tag{6}$$

with the smoothly varying c_i the Boussinesq-type approximations of the wave celerity of the components. Inserting this decomposition and decomposition (4) in the model equations (1) and (2), and neglecting the right-hand side of (2), the following characteristic equations are satisfied approximately by each component:

$$\mathbf{i}_i^{\perp} \cdot \partial\overline{\mathbf{u}}_i \approx 0 \ , \text{ along } \frac{d\mathbf{x}}{dt} = \overline{\mathbf{u}} \ , \tag{7}$$

$$c_i \partial H_i \pm H\mathbf{i}_i \cdot \partial\overline{\mathbf{u}}_i \approx 0 \ , \text{ along } \frac{d\mathbf{x}}{dt} = \overline{\mathbf{u}} \pm c_i\mathbf{i}_i \ , \tag{8}$$

with the unit vectors $\mathbf{i}_i$ and $\mathbf{i}_i^{\perp}$ defined by $\mathbf{i}_i = \mathbf{k}_i/|\mathbf{k}_i|$ and $\mathbf{i}_i^{\perp} \cdot \mathbf{i}_i = 0$. Since decomposition (4) implies that a wave component propagates only in the direction $\overline{\mathbf{u}} + c_i\mathbf{i}_i$, *no* information concerning wave component i propagates in the directions $\overline{\mathbf{u}}$ and $\overline{\mathbf{u}} - c_i\mathbf{i}_i$. This important key element will be used later. Note that one could also include in (4) components that move with the flow velocity $\overline{\mathbf{u}}$ in the presence of currents (no information propagating in the directions $\overline{\mathbf{u}} \pm c_i\mathbf{i}_i$), but this has not been considered so far.

The assumption is now made that on average the solution near a boundary can be characterized locally by one incoming wave component (superscript $+$) and one outgoing wave component (superscript $-$):

$$\partial H \approx \partial H^+ + \partial H^- \ , \ \partial\overline{\mathbf{u}} \approx \partial\overline{\mathbf{u}}^+ + \partial\overline{\mathbf{u}}^- \ . \tag{9}$$

The angle with respect to the inward normal at the boundary and the celerity of these two wave components are respectively θ^+ and c^+, and θ^- and c^- (cf. Figure 1). Restricting ourselves to variations in time, we obtain from (7) and (8), substituting $\mathbf{i}^+ = (\cos\theta^+, \sin\theta^+)^{\mathrm{T}}$ and $\mathbf{i}^- = (\cos\theta^-, \sin\theta^-)^{\mathrm{T}}$, and denoting velocity components in normal and tangential direction by the subscripts n and s:

$$-\sin\theta^+\frac{\partial\overline{u}_n^+}{\partial t} + \cos\theta^+\frac{\partial\overline{u}_s^+}{\partial t} = 0 \ , \ c^+\frac{\partial H^+}{\partial t} - H\left(\cos\theta^+\frac{\partial\overline{u}_n^+}{\partial t} + \sin\theta^+\frac{\partial\overline{u}_s^+}{\partial t}\right) = 0 \ , \tag{10}$$

$$-\sin\theta^-\frac{\partial\overline{u}_n^-}{\partial t} + \cos\theta^-\frac{\partial\overline{u}_s^-}{\partial t} = 0 \ , \ c^-\frac{\partial H^-}{\partial t} - H\left(\cos\theta^-\frac{\partial\overline{u}_n^-}{\partial t} + \sin\theta^-\frac{\partial\overline{u}_s^-}{\partial t}\right) = 0 \ . \tag{11}$$

Combining the second equation of (11) with (9) we immediately obtain:

$$c^-\frac{\partial H}{\partial t} - H\left(\cos\theta^-\frac{\partial\overline{u}_n}{\partial t} + \sin\theta^-\frac{\partial\overline{u}_s}{\partial t}\right) = c^-\frac{\partial H^+}{\partial t} - H\left(\cos\theta^-\frac{\partial\overline{u}_n^+}{\partial t} + \sin\theta^-\frac{\partial\overline{u}_s^+}{\partial t}\right) \ . \tag{12}$$

This is the basis of our flexible boundary procedure.

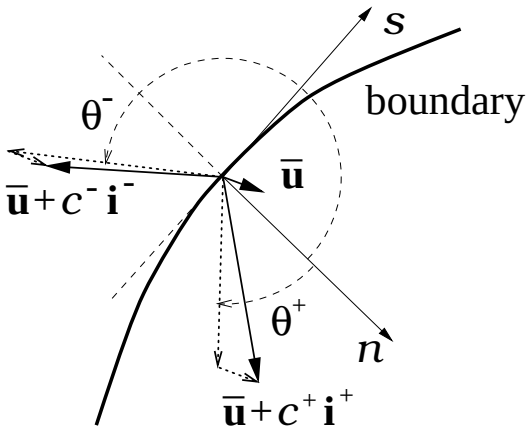

FIG. 1. Incoming and outgoing wave component at boundary

THE BOUNDARY CONDITION

By imposing at the boundaries the combination of variables in the left-hand side of (12), we specify only the incoming wave as is evidenced by the right-hand side. This incoming wave can be set to zero (open non-reflecting boundary) or be set to the specified incident wave (open seaward boundary). It may also be set equal to a part of the outgoing wave to model reflection:

$$\frac{\partial H^+}{\partial t} = r\frac{\partial H^-}{\partial t}\ ,\ \frac{\partial \overline{u}_n^+}{\partial t} = -r\frac{\partial \overline{u}_n^-}{\partial t}\ ,\ \frac{\partial \overline{u}_s^+}{\partial t} = r\frac{\partial \overline{u}_s^-}{\partial t}\ , \tag{13}$$

with r the (wave-dependent) reflection coefficient.

Boundary conditions are obtained by eliminating H^+, $\overline{u}_n^+$, and $\overline{u}_s^+$ in the right-hand side of (12) using one of the above methods. The result is a condition formulated in terms of *time derivatives* of the unknowns. Because of the approximations involved, this could lead to solutions drifting away. To compensate for this effect, we include a small correction term that forces the solution on average to be equal to the value imposed. Using (10) to write the right-hand side of (12) in terms of the water elevation of the incoming wave, the boundary condition to be imposed at an incident wave boundary then reads:

$$\frac{\partial H}{\partial t} - \frac{H}{c^-}\left(\cos\theta^- \frac{\partial \overline{u}_n}{\partial t} + \sin\theta^- \frac{\partial \overline{u}_s}{\partial t}\right) = \left(1 - \frac{c^+}{c^-}\cos(\theta^+ - \theta^-)\right)\frac{\partial \zeta_{\rm giv}}{\partial t} + \epsilon_{\rm corr}\omega^+(\zeta_{\rm giv} - \zeta)\ , \tag{14}$$

with $\zeta_{\rm giv}$ the imposed water elevation, c^+ and ω^+ the mean celerity and mean frequency of the imposed wave, and with $\epsilon_{\rm corr} \ll 1$ a small coefficient that determines the magnitude of the correction term. Likewise, we obtain the condition for a partially reflecting boundary by evaluating the right-hand side of (12) using (13), (10), and (11):

$$\frac{1-r}{1+r}\frac{\partial H}{\partial t} - \frac{H}{c^-}\left(\cos\theta^- \frac{\partial \overline{u}_n}{\partial t} + \frac{1-r}{1+r}\sin\theta^- \frac{\partial \overline{u}_s}{\partial t}\right) = \epsilon_{\rm corr}\omega^+ \frac{H}{c^-}\cos\theta^- \overline{u}_n\ . \tag{15}$$

For $r = 0$ (no reflection) the left-hand side of this equation is equal to that of (14); the difference in right-hand sides is due to the absence of an imposed incident wave

and a different correction term ensuring here on average zero discharge through the boundary. For $r = 1$ (full reflection) the equation simplifies to $\partial \overline{u}_n / \partial t = -\epsilon_{\text{corr}} \omega^+ \overline{u}_n$ or $\overline{u}_n = 0$, as expected.

Remaining Boundary Equations

The system of four partial differential equations (1), (2), and (3) requires a total of four equations at the boundary for the determination of the four unknowns H, $\overline{\mathbf{u}}$ (two components), and $\widetilde{H}$. The first one is the boundary condition for the incoming wave described above, while the second one is formed by the characteristic equation describing the propagation of the outgoing wave toward the boundary. This equation is obtained by taking the sum of c^+ times the continuity equation, $-H \cos\theta^+$ times the normal momentum equation, and $-H \sin\theta^+$ times the tangential momentum equation. According to the second equation of (10), this combination does not contain any information about the incoming wave.

The third equation describes the $\overline{\mathbf{u}}$ characteristic and is associated with the flow (cf. Eq. 7). A complicating factor is that, due to the orbital motion, this information is both incoming and outgoing within a wave cycle. At present we use the tangential momentum equation, which is a rather weak condition and based on the assumption that the flow is normal to the boundary and outgoing. To avoid unstable behavior when the flow in incoming, the correction term $-\epsilon_{\text{corr}} \omega^+ \overline{u}_s$ is added to the right-hand side. Despite its ad hoc nature this procedure works remarkably well, although the results indicate that there is a certain need for improvement. A more accurate but also more complicated procedure would be one where the momentum equation normal to the flow direction is used when the flow is outgoing, and the flow direction is imposed when the flow is incoming, with a smooth transition between both equations when the flow direction normal to the boundary changes. Such a procedure will also be suited for wave problems with currents.

The fourth equation is the boundary condition for auxiliary variable $\widetilde{H}$ (Eq. 3). At a fully reflecting boundary the symmetry condition $\partial \widetilde{H} / \partial n = 0$ can be applied. In all other situations it is impossible to derive an adequate condition for $\widetilde{H}$ without knowledge of the wave pattern at the boundary. Yet such a condition is essential, to avoid violation of the conditions (5). The boundary condition for $\widetilde{H}$ that we apply at present consists of Eq. 3, but with the second derivatives normal to the boundaries replaced by the approximations $\partial^2 \widetilde{H} / \partial n^2 = \partial^2 (\widetilde{\zeta} + h) / \partial n^2 \approx -k_{\text{typ},n}^2 \widetilde{\zeta} + \partial^2 h / \partial n^2 = -k_{\text{typ},n}^2 (\widetilde{H} - h) + \partial^2 h / \partial n^2$ (similar for H), with $k_{\text{typ},n}$ the normal component of a typical wave number vector. At boundaries with imposed, and hence known incident wave, it would be possible to adjust $k_{\text{typ},n}$ dynamically. The accuracy of the $\widetilde{H}$ boundary condition at other boundaries is less critical, because the dynamic determination of c^- described in the next section compensates automatically for approximation errors.

Determination of c^- and θ^-

The characteristic variables of the incoming wave (celerity c^+ and direction θ^+) are either obtained from the imposed wave signal (incident wave, cf. Eq. 14), or determined by the reflected outgoing wave in which case we have $c^+ = c^-$ and $\theta^+ = \pi - \theta^-$

(reflecting wave, cf. Eq. 15). The parameters c^- and θ^- in the boundary conditions are determined dynamically from (11), by solving these equations for the unknowns $\cos\theta^- c^-$ and $\sin\theta^- c^-$, i.e.:

$$\cos\theta^- c^-\Big|^n = \frac{b^n}{a^n}\ ,\ \sin\theta^- c^-\Big|^n = \frac{c^n}{a^n}\ , \tag{16}$$

with:

$$\begin{aligned}
a^n &= \delta\left(\frac{\partial H^-}{\partial t}\frac{\partial H^-}{\partial t} + \left(\epsilon_{\rm typ}\omega^-_{\rm typ}Z^-_{\rm typ}\right)^2\right) + (1-\delta)a^{n-1}\ ,\\
b^n &= \delta\left(\frac{\partial H^-}{\partial t}H\frac{\partial \overline{u}^-_n}{\partial t} + \cos\theta^-_{\rm typ}c^-_{\rm typ}\left(\epsilon_{\rm typ}\omega^-_{\rm typ}Z^-_{\rm typ}\right)^2\right) + (1-\delta)b^{n-1}\ ,\\
c^n &= \delta\left(\frac{\partial H^-}{\partial t}H\frac{\partial \overline{u}^-_s}{\partial t} + \sin\theta^-_{\rm typ}c^-_{\rm typ}\left(\epsilon_{\rm typ}\omega^-_{\rm typ}Z^-_{\rm typ}\right)^2\right) + (1-\delta)c^{n-1}\ ,
\end{aligned} \tag{17}$$

where superscript n denotes the discrete time level. The time derivates of the flow variables in the above expressions are evaluated at time level n, and pertain to the outgoing wave. They are obtained either by subtracting the incident wave signal from the solution of the Boussinesq-type equations at the boundary, or by formulating them in terms of that solution combining (13) with (9). To satisfy the conditions (5) underlying the entire boundary procedure, a strong underrelaxation is applied ($\delta \ll 1$) which ensures that c^- and θ^- vary indeed smoothly in time. Furthermore, small terms are added to the coefficients in (17) with typical outgoing wave amplitude $Z^-_{\rm typ}$, typical outgoing wave frequency $\omega^-_{\rm typ}$, and small parameter $\epsilon_{\rm typ} \ll 1$ to ensure that, in the absence of an outgoing wave, c^- and θ^- get the typical values $c^-_{\rm typ}$ and $\theta^-_{\rm typ}$.

RESULTS

The properties of the proposed boundary procedure have been evaluated by considering the propagation of unidirectional, monochromatic waves over a uniform bottom. Reference solutions obtained for a square domain measuring 4.5 by 4.5 wave lengths were compared with results obtained for the rectangular domain consisting of the left 2 wave lengths of this square. Imposing the wave at the left and lower boundary, the difference between both solutions over the lower 2 wave lengths of the rectangular domain (a square of 2 by 2 wave lengths) is then, within a certain time slot, entirely due to spurious reflections at the right boundary of the rectangular domain. Insight in the behavior of the boundary procedure applied at that boundary is obtained by calculating this difference for a number of waves, varying direction, period, as well as amplitude. The reflection coefficient r is obtained by normalizing this difference, taking the average of the difference in wave elevation over all grid points within the small square. This has been done at a late enough time level for spurious reflections to have spread over the entire small square. The same test has been considered in (Borsboom et al. 2000) to evaluate the previous version of the present boundary procedure, and is similar to the test described in (Van Dongeren and Svendsen 1997).

Table 1 summarizes the results that have been obtained. The characteristics of the incident wave are specified in terms of the direction (θ), the ratio of wave amplitude and water depth (a/h), and the product of wave number and water depth (kh). The

TABLE 1. Average reflection coefficients

$a/h = 0.02$, $kh = 1.11$		$kh = 1.11$, $\theta = 20°$		$\theta = 20°$, $a/h = 0.02$	
θ	r	a/h	r	k/h	r
20°	0.006	0.02	0.006	2.07	0.013
45°	0.004	0.10	0.016	1.11	0.006
70°	0.008			0.18	0.006

results of Table 1 have been obtained with the following setting: dispersion parameter $\alpha = 0.395$ in Eq. 3; angle θ^+ in the incident wave boundary condition (14) applied at the lower and left boundary set equal to the wave angle; angle θ^+ in the open boundary condition (15) applied at the upper and right boundary set equal to zero where we specified a zero reflection coefficient ($r = 0$); $\epsilon_{\rm corr} = 0.01$ was used in all boundary conditions; $\delta = 0.001$ and $\epsilon_{\rm typ} = 0.1$ were used in the expressions (17), with $\omega^-_{\rm typ}$, $Z^-_{\rm typ}$, $\theta^-_{\rm typ}$, and $c^-_{\rm typ}$ set equal to the values pertaining to the incident wave. In order to appreciate the value of δ (the relaxation coefficient per time step), it should be mentioned that the number of time steps per wave period was about 50. This number varies because of the Courant condition that is based on the long-wave celerity $\sqrt{gh}$, while the smaller celerities of the modeled waves depend on the wave period. 40 grid points per wave length were used.

The general behavior of the reflection error in Table 1 is the same as reported in (Borsboom et al. 2000), but the overall level of the error, that was already quite small, is significantly lower. The reflection error is larger for higher-frequency waves (larger value of kh), which is probably related to the approximate boundary condition that we use for $\widetilde{H}$. As expected, the reflection error also increases with larger amplitude (larger value of a/h). The applied method compensates for nonlinear effects, but does not include them all which is virtually impossible. The reflection error is fairly insensitive to the wave angle.

In the computations described above $\theta^-_{\rm typ}$ has been taken equal to the angle that the incident wave would have at a particular boundary. Since the wave form changes during the propagation through the domain (especially when nonlinear effects are large), the dynamically determined θ^- will generally not be exactly equal to $\theta^-_{\rm typ}$ but still be very close. A more severe test is therefore a computation with $\theta^-_{\rm typ}$ set to $-180°$. This 'neutral' value of a typical angle of the outgoing wave (note that angles are defined with respect to the *inward* normal) will often be the best possible estimation.

Figure 2 shows the wave field and reflection pattern for a large-amplitude wave at 20° angle when $\theta^-_{\rm typ}$ is set to $-180°$. One observes the rapid steepening of the wave crests and flattening of the waves at the troughs. Also, perturbations enter the domain, especially from the lower boundary, due to the mismatch between the imposed monochromatic incident wave and the nonlinearities developing inside the domain. As expected, the spurious reflection consists mainly of a small part of the higher harmonics generated by the incident wave, reflected at an angle of 20° from the right boundary. The same behavior was observed in the other computations. This means that measuring the reflection coefficient by averaging the reflected wave over the entire domain gives a

rather optimistic value for waves at a large angle of incidence. When this is taken into account when interpreting the values in the second column of Table 1, the conclusion indeed reads that the amplitude of the reflected wave increases with the angle of the incident wave, which is undoubtedly due to the approximate boundary condition for the $\overline{\mathbf{u}}$ characteristic. That boundary condition is probably also responsible for the comparatively large distortion close to the boundary.

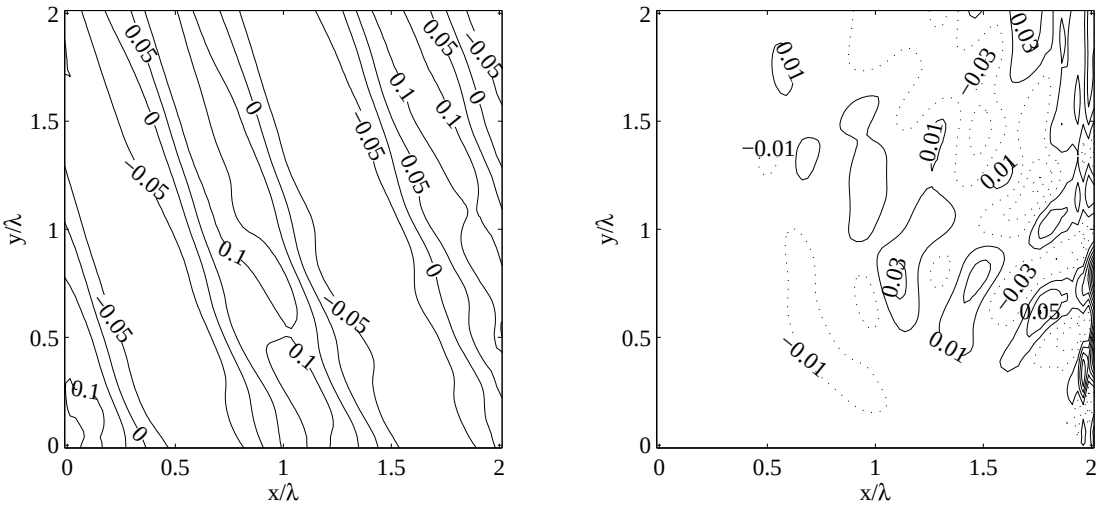

FIG. 2. Solution and reflection error relative to wave amplitude for wave at $20°$ **angle,** $kh = 1.11$**, and** $a/h = 0.1$ **after 7.3 wave periods.**

Figure 3 shows the behavior in time of c^- and θ^- halfway the right boundary. After about two wave periods, when the incident wave reaches that location, the values start to deviate from the specified typical values c^-_{typ} and θ^-_{typ}. Due to the applied underrelaxation, in combination with the smooth increase of the incident wave amplitude over three wave periods, the adaptation takes place gradually. The results show that it takes only slightly more than two wave periods for c^- and θ^- to reach their final value. The outgoing wave angle converges very well to the expected value $20° - 180°$. The celerity of the outgoing wave reaches a value slightly lower than than of the incident wave due to the developed higher harmonics.

CONCLUDING REMARKS

We have described a method that allows to control the reflection at boundaries by analysing dynamically the local wave pattern. The method has been tested for monochromatic waves at straight non-reflecting boundaries. The results show very low spurious reflections of only about 1% for waves at different angles, periods, and amplitudes. Future work will include validation of the method for irregular waves and irregular boundaries which due to the larger complexity will probably lead to larger reflection errors. On the other hand, one result indicates that the method is capable of adapting rather quickly to changes in the outgoing wave pattern. We therefore expect to find reflections low enough to be acceptable in applications. The modeling of wave-dependent partial reflection will be investigated as well, using the angle and celerity of the outgoing wave already determined.

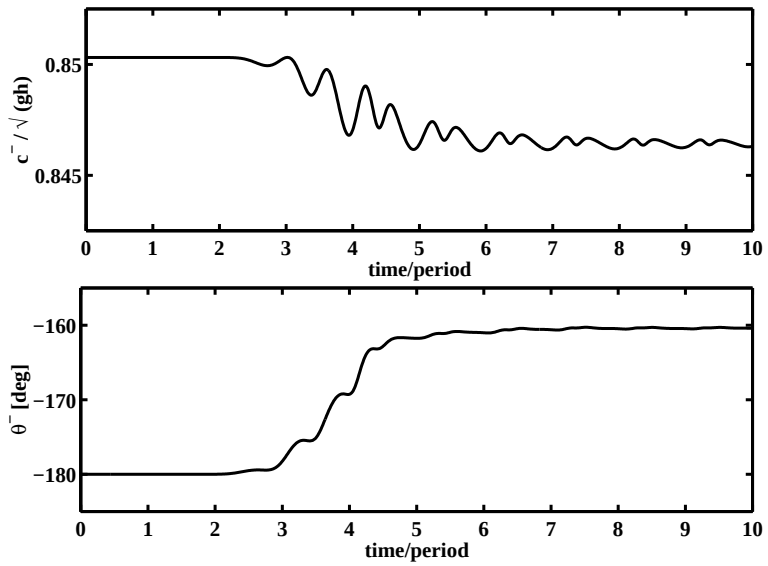

FIG. 3. Dynamic determination of c^- and θ^- for wave solution of Figure 2.

The method presented in this paper is a substantial improvement over the method briefly described in (Borsboom et al. 2000) that already performed quite well. This is mainly due to the fact that we now use variables that are strictly evaluated at boundaries instead of at some distance from the boundaries, to dynamically determine the behavior of the outgoing wave. Besides being more accurate, the upgraded procedure also turns out to be easier to implement, while the modeling of partial reflection can be incorporated easily. These advantages, together with the increased robustness, were the main motivation for the present development.

REFERENCES

Borsboom, M., Doorn, N., Groeneweg, J., and Van Gent, M. 2000. A Boussinesq-type wave model that conserves both mass and momentum. *Proc. 27th Int. Conf. on Coastal Engrg.*, B. L. Edge, ed., Vol. 1. ASCE, 148–161.

Borsboom, M., Doorn, N., Groeneweg, J., and Van Gent, M. 2001. Near-shore wave simulations with a Boussinesq-type model including breaking. *Proc. 4th Int. Conf. On Coastal Dyn.*, H. Hanson and M. Larson, eds. ASCE, 759–768.

Givoli, D. 1991. Non-reflecting boundary conditions. *J. Comput. Phys.*, 94, 1–29.

Luchini, P. and Tognaccini, R. 1996. Direction-adaptive nonreflecting boundary conditions. *J. Comput. Phys.*, 128, 121–133.

Madsen, P. A. and Sørensen, O. R. 1993. Bound waves and triad interactions in shallow water. *Ocean Engrg.*, 20, 359–388.

Van Dongeren, A. R. and Svendsen, I. A. 1997. Absorbing-generating boundary condition for shallow water models. *J. Wtrwy., Port, Coast., and Oc. Engrg.*, 123, 301–313.

Wei, G., Kirby, J. T., and Sinha, A. 1999. Generation of waves in Boussinesq models using a source function method. *Coastal Engrg.*, 36, 271–299.

Key Words

Title: FLEXIBLE BOUNDARY CONDITIONS FOR A BOUSSINESQ-TYPE WAVE MODEL

absorbing boundary condition

boundary conditions

Boussinesq-type model

numerical modeling

reflection

wave propagation